I. J. Computer Network and Information Security, **2023, 4, 1-12**
Published Online on August 8, 2023 by MECS Press (http://www.mecs-press.org/)
DOI: 10.5815/ijcnis.2023.04.01

Performance Analysis of 5G New Radio LDPC over Different Multipath Fading Channel Models

Mohammed Hussein Ali*
Electrical Engineering Department, Faculty of Engineering, Mustansiriyah University, Baghdad, Iraq
E-mail: eeph005@uomustansiriyah.edu.iq
ORCID iD: https://orcid.org/0000-0002-2516-4066
*Corresponding author

Ghanim A. Al-Rubaye
Electrical Engineering Department, Faculty of Engineering, Mustansiriyah University, Baghdad, Iraq
E-mail: g.a.m.al-rubaye@uomustansiriyah.edu.iq
ORCID iD: https://orcid.org/0000-0001-5412-5157

Received: 18 September 2022; Revised: 12 December 2022; Accepted: 01 March 2023; Published: 08 August 2023

Abstract: The creation and developing of a wireless network communication that is fast, secure, dependable, and cost-effective enough to suit the needs of the modern world is a difficult undertaking. Channel coding schemes must be chosen carefully to ensure timely and error-free data transfer in a noisy and fading channel. To ensure that the data received matches the data transmitted, channel coding is an essential part of the communication system's architecture. NR LDPC (New Radio Low Density Parity Check) code has been recommended for the fifth-generation (5G) to achieve the need for more internet traffic capacity in mobile communications and to provide both high coding gain and low energy consumption. This research presents NR-LDPC for data transmission over two different multipath fading channel models, such as Nakagami-m and Rayleigh in AWGN. The BER performance of the NR-LDPC code using two kinds of rate-compatible base graphs has been examined for the QAM-OFDM (Quadrature Amplitude Modulation-Orthogonal Frequency Division Multiplexing) system and compared to the uncoded QAM-OFDM system. The BER performance obtained via Monte Carlo simulation demonstrates that the LDPC works efficiently with two different kinds of channel models: those that do not fade and those that fade and achieves significant BER improvements with high coding gain. It makes sense to use LDPC codes in 5G because they are more efficient for long data transmissions, and the key to a good code is an effective decoding algorithm. The results demonstrated a coding gain improvement of up to 15 dB at 10^{-3} BER.

Index Terms: QAM-OFDM, NR-LDPC, Nakagami-m Fading Channel, BER Performance, Rician Fading Channels, Turbo Codes (TCs), 3rd Generation Partnership 5G NR, Rayleigh Fading Channel, Line of Sight (LOS), AWGN.

1. Introduction

The AWGN noise, multipath fading, and interference, all contribute to a communication channel's error rate. The original data flow is corrupted by channel impairments, thus the data received is not identical to the data supplied. Channel coding is employed to mitigate the defects that occur during information transfer. This indicates that the original flow of information is subjected to a sequence of algorithmic processes on the transmitter side (channel encoding). Channel decoding on the recipient side is done by implementing various processes that are designed to correct errors. The selection of an appropriate coding system is clearly critical to the speed and reliability of transmitting data. The coding system should be flexible, have minimum complexity of computation, low latency, provide good reliability, and taken in account the low cost [1,2].

In the 1960s, Rober Gallager [3] presented LDPC for the first time in his Doctoral dissertation at MIT. As a result of its many attractive features, LDPC codes have gained considerable interest in recent years. Real-time, high-throughput connections are possible thanks to the selection of these codes. One, the LDPC-based technique is capacity-approaching; two, these codes may be efficiently decoded by parallel iterative decoding algorithms with minimal delay [4]. Researchers are now looking into LDPC to assess its capabilities for future software design [5]. The LDPC codes feature a completely parallelizable decoding implementation and are structurally simpler than other iterative code such as turbo codes [6]. Generally, turbo codes (TCs) have complex code structure, and large delay in the process of decoding and that make TC unsuitable for 5G. LDPC codes use less bandwidth and perform better for larger lengths of

blocks. LDPC codes are also more efficient than other codes [7].

The encoding difficulty of LDPC codes is larger than that of turbo codes and is inherently quadratic in the code dimension, however it is possible to lower this complexity. It has been shown that LDPC codes may get very near to the channel capacity. In particular, MacKay demonstrated via his study of random coding that LDPC code sembles may rapidly approach the Shannon capacity limit as a function of the code's length, and that errors in such codes are almost detectable [8,9]. Studies on LDPC codes have been found to have irregular and coding at multiple levels. There are just a handful of studies on the topic of Rayleigh and Rician fading channels [7, 10]. LDPC codes with iterative soft-decision decoding achieves performance very close to the Shannon limit, lower decoding complexity and it is easy to modify the code rates with better BER performance than TCs [11]. When compared to LDPC codes, TCs have many advantages, including reduced encoder complexity, fewer decoder iterations, and less connectivity in the trellis graph, all of which may have a beneficial effect on latency. In addition, puncturing in the TC encoder may further reduce complexity. Tanner graphs with no four-cycle girths may be formed by LDPC codes built using either random or algebraic construction methods. So, until it finds the right code, the decoding algorithm must do numerous iterations (large latency). It follows that the LDPC code's will have better BER performance in comparison to that of the TC [11, 12].

In this work, we design and constructed an NR-LDPC-QAM-OFDM system, and we assess and compare its BER performance to that of uncoded QAM-OFDM systems over a Multipath Rayleigh environment, and a Multipath Nakagami-m environment in AWGN. The obtained results demonstrate that the NR-LDPC-COFDM system outperforms the uncoded OFDM system in a multipath channel situation where the channels gradually degrade. The number of iterations needed for LPDC-OFDM to converge is bigger, which is a major drawback, the NR-LDPC can reducing up to 16–24 % of the decoding iterations required to correct the channel errors at relatively low signal-to-noise ratio. The throughput varied from 20 to 200 Gbps across all of the analyzed submatrix sizes, which is more than enough to fulfill the throughput requirement of the 5G New Radio (NR) standard.

2. Related Works

According to 3rd Generation Partnership 5G NR standardization project (3GPP), LDPC a coding strategy for data channels is being considered [13]. For improved mobile broadband (MBB), LDPC codes have recently been selected as the 5G New Radio (NR) channel coding method [14].

Error-correction performance of 5G LDPC codes has been improved by several techniques in recent years [15–19]. In [15], adjusted minimum sum (MS) and generalized approximate-min algorithms were presented in [16]. By taking into consideration the approximate-min method [17]. Non-linear functions, like the BP decoding, need a substantial amount of implementation complexity. To simplify the non-linear functions in the BP method, the authors of [18], presented a hybrid decoding technique. To improve the accuracy of the calculations, the authors of [19] insert the offset and normalization factors into decoding at different times, with values that are adjusted using machine learning.

In order to make the most of the available spectrum, the OFDM communication system is a useful technique. In this setup, using M-QAM might greatly boost the spectrum utilization rate. However, high-order modulation can lead to a significant error rate for low-power transmission systems in some situations. Forward Error Correction (FEC) are frequently used to reduce the number of errors in an ODFM system [20]. OFDM is often used along with a cyclic prefix (CP), in order to remove inter-symbol interference (ISI), which transforms the frequency-selective multipath into narrow band frequency-flat channels [21].

Channel models for multipath propagation are described in Section III. In Section IV, we present our model of NR-LDPC - OFDM system. Details of the BER computation over Nakagami-m fading channel In Section V. The simulation results used to assess LDPC- OFDM systems' performance are shown in Section VI. We have compared the computational complexity as well. The conclusion and references are provided in the last section.

3. Communication Channel Models

The assumption of some level of noise distortion in transmitted signals is central to the study of communication theory. Typically, it is assumed that the noise is additive, white, and follows a Gaussian distribution. The availability of many paths between transmitters and receivers is a more real scenario for wireless links. These paths can be either direct or created by reflection, diffraction, or scattering. Vectors of independent delayed signals, each with a different frequency and amplitude and delay, compose the total received signal. [22, 23].

The fading envelope of wireless signals may be described using the Rayleigh and Rician distributions for localized or temporary fades, and the lognormal distribution for more widespread phenomena. However, Nakagami's m-distribution [24], is a more flexible statistical model that can simulate not only the Rayleigh but also the one-sided Gaussian fading environment. In addition, the Nakagami distribution may provide a good approximation to the log-normal and Rician distributions for certain ranges of mean rating scale [11, 21, 25].

For small signal-to-noise ratios (SNR), the match between the Nakagami and Rician distributions is more precise than for large SNRs. In addition, the Nakagami distribution is more adaptable than the log-normal and Rician distributions [11, 25-27], and provides a better match to experimental data for a wide variety of physical propagation of

the channels. Fading will have a significant impact on a system's performance.

3.1. Rayleigh Fading Channel

The most common model for narrowband transmission across wireless and mobile channels is the flat fading channel. The flat fading channel attenuates all components of the signal frequency by the same factor. For the received signal in the complex baseband form may thus be represented as [11, 21]

$$y = \alpha x + w \tag{1}$$

where y is the received symbol and x is the symbol on the broadcast channel, w is the amplitude of the AWGN, and α is the fading amplitude. The amplitude of fade, denoted by " α," is a stochastic function. Without any fading at all (α = 1), the channel is just AWGN. The symbols r = { I, Q } represent the real and imaginary parts, respectively.

The Rayleigh fading channel happens when there are several indirect pathways between the transmitting and receiving ends. There is no direct line of sight (LOS). The worst-case scenario is Rayleigh fading. This form of fading may be dealt with analytically, which gives insight into hard conditions in the field of wireless communication, like downtown urbanized settings.

If the magnitude of the fading channel follows the Rayleigh distribution, then the distribution $P(|\alpha|)$ can be expressed as [28]

$$f(\alpha) = \frac{\alpha}{\sigma_h^2} \exp\left(-\frac{\alpha^2}{2\sigma_h^2}\right) \tag{2}$$

In this case, the distribution of the inphase component and the quadrature phase component will follow the Gaussian distribution with zero mean and σ_h^2 = ½ as

$$f_\alpha(\alpha^I) = \frac{1}{\sqrt{2\pi\sigma_h^2}} \exp\left(-\frac{(\alpha^I)^2}{2\sigma_h^2}\right), \quad -\infty \le \alpha^I < \infty \tag{3}$$

$$f_\alpha(\alpha^Q) = \frac{1}{\sqrt{2\pi\sigma_h^2}} \exp\left(-\frac{(\alpha^Q)^2}{2\sigma_h^2}\right), \quad -\infty \le \alpha^Q < \infty \tag{4}$$

where σ_h^2 represent the average power of received signal, which is a function of the of path loss as will as shadowing alone.

3.2. Nakagami-m Fading Channel

As a distribution, the Nakagami - m combines the best features of the Rayleigh and Rician distributions. Although Rayleigh and Rician distributions are often employed to characterize the mobile communication channel, the Rayleigh distribution fails to capture long-distance fading effects with satisfactory accuracy [11, 21, 24].

When compared to the Rayleigh and Rician models, Nakagami offers a more thorough justification to both less and more extreme circumstances than the Rayleigh and Rican model, which improves fit to the data from a mobile communication channel. It is considered that Nakagami-m is a generalization of Chi-distribution. It is closely related to chi squared with 2m degrees of freedom in mathematics [29].

Nakagami-m also provides the optimum match for radio wave propagation from satellites to buildings and vice versa. In this scenario, we utilize a parameter known as the m parameter or shape parameter to characterize the level of fading. This parameter gives us an idea of how much fading is caused by scattering and multipath interference. Hence, the magnitude of the fading channel in the time domain follows the Nakagami-m distribution and is defined as [11, 21]:

$$f_\alpha(\alpha) = \frac{2m^m}{\Gamma(m)\Omega^m} \alpha^{2m-1} \exp\left(-\frac{m\alpha^2}{\Omega}\right), \quad 0 \le \alpha < \infty \tag{5}$$

Where, Γ (.) is the gamma function and $\Omega = \mathrm{E}(r^2) = 2\sigma^2$ is multipath scatter field average power The strength of the signal that was received is denoted by the symbol " α ". The shape parameter is m and (m≥ 0.5), and when m = 1, the Nakagami-m distribution degenerates to the Rayleigh distribution, where is the inverse of the normalized variance of α^2. When modeling Land-mobile and indoor mobile multipath propagation, this distribution is frequently the best match. In this case, $\alpha = \alpha^I + j\alpha^Q$, where $\alpha^I = |\alpha| \cos(\theta)$ and $\alpha^Q = |\alpha| \sin(\theta)$.The distribution of the inphase component and the quadrature phase component can be expressed as

$$f_\alpha(\alpha^I) = \frac{2m^m}{\Gamma(m)|\cos(\theta)|\Omega^m} \left(\frac{\alpha^I}{\cos(\theta)}\right)^{2m-1} \exp\left(-\frac{m(\alpha^I)^2}{\Omega\cos(\theta)^2}\right), \quad -\infty \le \alpha^I < \infty \tag{6}$$

$$f_{\alpha}(\alpha^{Q}) = \frac{2m^{m}}{\Gamma(m)|\sin(\theta)|\Omega^{m}} \left(\frac{\alpha^{Q}}{\sin(\theta)}\right)^{2m-1} \exp\left(-\frac{m(\alpha^{Q})^{2}}{\Omega \sin(\theta)^{2}}\right), \quad -\infty \leq \alpha^{Q} < \infty \tag{7}$$

4. 5G NR LDPC-OFDM System Model

Every possible channel in the physical world introduces unwanted noise, which in turn causes errors and lowers the system's dependability. Channel coding, which enhances the robustness of digital communication systems by including redundancies in the transmitted data in a managed fashion, [30]. The parity-check matrices of these codes, from which their name derives, consist mostly of zeros (or "0's") and just slightly more ones (1's). Visualizations and descriptions of LDPC codes are possible using matrices or using (Tanner graphs). There are two types of LDPC codes, regular and irregular. A protograph is referred to as a base graph in the 5G standard [31], whose utilization is based on coding rate or the number of information bits, To illustrate this, Fig.1 displays a scatter map of the base graph for the BG1 and BG2 matrices. Using Fig. 1, we can see that BG 1 in 5G LDPC has a size of (46 x 68) and a 1/3 a main code rate. BG2, with a dimension of 42 by 52 and 1/5 a main code rate of, is structurally comparable to Base Graph 1. There are 22 information bits in the first 10 columns of BG1, and 10 in the first 10 columns of BG2. It is important to keep in mind that the first two columns of both base graphs are always punctured and do not contribute to the transmission. By swapping out every zero-valued element in the base graph with a ($Z_c \times Z_c$) all-zero matrix and every non-zero-valued entry with a ($Z_c \times Z_c$) permutation matrix, it is possible to create a parity check matrix of protograph codes. Z_c is called lifting size, and refers to the number of attached copies of the protograph, usually denoted by the variable Z_c.

As protograph codes, LDPC codes might be regarded. The fact that each permutation is represented by a single integer when using a circularly-shifted identity matrix as a permutation matrix is one of its key advantages. [32].

The algorithmic efficiency of LDPC codes is significantly affected by the degree of sparsity in the underlying graph structure. [33].

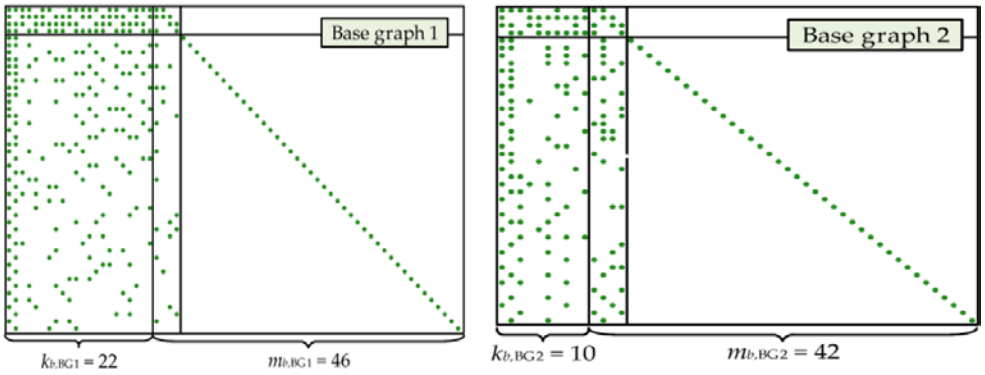

Fig.1. 5G NR-LDPC base graphs

To accommodate different block lengths and coding schemes, 5G NR employs two basic graphs and eight sets of modeling shift coefficient matrices for each base graph in the 5G standard, and as shown in Table 1, there are 51 various lifting sizes are specified.

Table 1. 5G LDPC code lifting sizes as a function of shift-value sets

Set index	a	lifting size $Z_c = 2 \times a^j$
0	2	{2, 4, 8, 16, 32, 64, 128, 256}, j∈ {0,1,2,3,4,5,6,7}
1	3	{3, 6, 12, 24, 48, 96, 192, 384 }, j∈ {0,1,2,3,4,5,6,7}
2	5	{5, 10, 20, 40, 80, 160, 320}, j∈ {0,1,2,3,4,5,6}
3	7	{7, 14, 28, 56, 112, 224}, j∈ {0,1,2,3,4,5}
4	9	{9, 18, 36, 72, 144, 288}, j∈ {0,1,2,3,4,5}
5	11	{11, 22, 44, 88, 176, 352}, j∈ {0,1,2,3,4,5}
6	13	{13, 26, 52, 104, 208}, j∈ {0,1,2,3,4}
7	15	{15, 30, 60, 120, 240}, j∈ {0,1,2,3,4}

BG1(with dimensions of 46 by 68) and BG2(with dimensions of 42 by 52) are the two kinds of rate-compatible base graphs for channel coding that have been finalized by the 3GPP. Both BG1 and BG2 are considered to be base graphs, and their structures are comparable. While BG1 is optimized for longer blocks (500≤ K≤ 8448) and higher rates (1/3 ≤R ≤8/9), BG2 is used for shorter blocks (40 ≤K ≤2560) and lower rates (1/5 ≤R ≤2/3) [34,35].

The degree of parallelism that may be used and the complexity of the related switch network are aspects that are taken into consideration when determining lifting sizes. It is important that supporting a variable code length may be

done effectively by simply selecting the right lifting size according on the amount of information that has to be encoded [31].

Our 5G New Radio (NR) LDPC-OFDM system architecture shown in Fig. 2. The irregular LPDC-PCM, is constructed according to the parameters (information block size K, coding rate R), are listed in five steps below. So, if the lifting size is Z, and the base graph has k_b columns of information, then $K = Z_c \times k_b$ is the nominal formula.

- First, choose the values of K and R by considering the basis graphs BG1 and BG2.

  BG1 k_b=22.
  BG2: k_b = 10 if K > 640, 9 if 560< K ≤640, 8 if 192< K ≤ 560, and 6 else.

- The second step is to calculate Z by selecting the lowest Z value from Table 1 such that $k_b \times Z_c \geq k$.
- The third step is to choose the shift coefficient matrix from Table 1 [Set index 0, Set index 1,..., Set 7] based on the lifting size Z.
- The fourth step is to use the modular Z operation, to determine the value of the shifting coefficient $S_{i,j}$ specified by Equation (5).
- The fifth step is to substitute each item in the final exponent matrix with the $(Z_c \times Z_c)$ permutation matrix or zero matrix. Finally, a PCM (H) of dimension $(m_b Z_c \times n_b Z_c)$ has been constructed, marking the end of the LDPC code construction.

$$S_{i,j} = f(B_{m,n}, z) = \begin{cases} -1 & if B_{m,n} = -1 \\ mod(B_{m,n}, z) & O.W \end{cases} \quad (8)$$

In 5G NR-LDPC codes, information bits are represented by the first 22 columns of base graph 1 and the first 10 columns of base graph 2. To emphasize, the first two columns of both base graphs are always punctured and never broadcast. So, n is the length of codeword. n = $66Z_1$ for LDPC BG 1 and n = $50Z_2$ for LDPC BG 2.

Finally, 5G NR-LDPC codes allow for rate matching during encoding operation, to control of transmitted bits to be chosen.

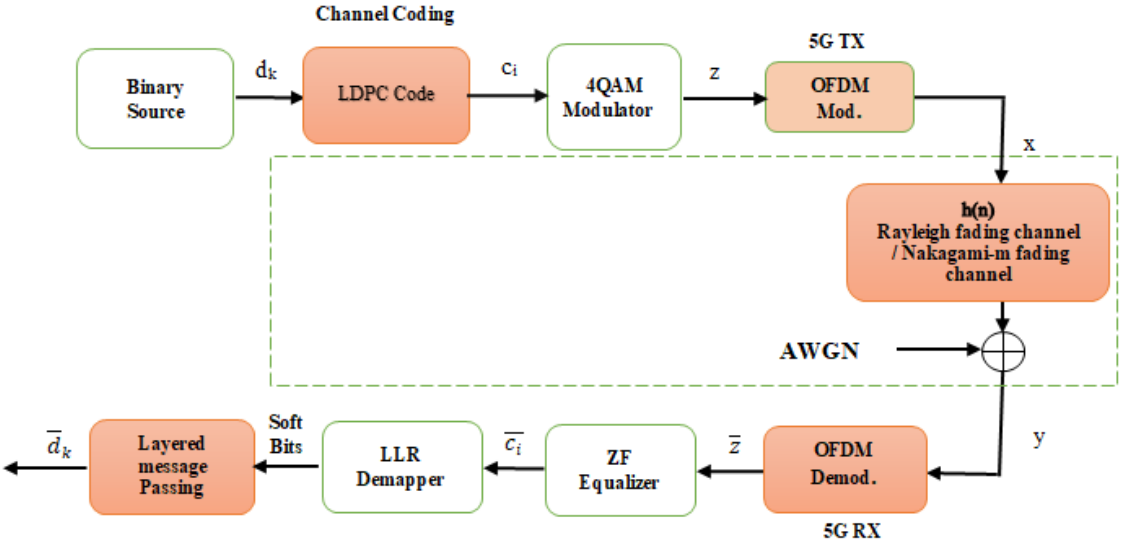

Fig.2. 5G New Radio LDPC-OFDM system architecture

Initial steps include utilizing the LDPC encoder to transform a block of information bits (d = d_0, d_1,..., d_{k-1}) into a codeword (c = c_0, c_1,..., c_{n-1}). The bits of the codeword c are then sorted into groups and mapped onto the 2^k symbols of a quadrature amplitude modulation (QAM) constellation, so that, for a k- tuple{ c_m, c_{m+1},... c_{m+k+1} } of bits which is corresponding QAM symbol is [11, 20, 21, 23]

$$X_k = \boldsymbol{C}[\sum_{m=0}^{k-1} 2^{k-1-m} c_m] \quad (9)$$

where $\boldsymbol{C} \in \mathbb{C}^{1X2^k}$ denotes the Gray-encoded vector in the time domain, a complex OFDM signal in baseband may be constructed using an N-points IFFT, as shown in [11, 21, 33,35].

$$x_n = \frac{1}{\sqrt{N}} \sum_{k=0}^{N-1} X_k \exp\left(\frac{2j\pi kn}{N}\right), n = 0,1, \dots, N-1 \quad (10)$$

Where N denotes the sub-carriers number.

IFFT transforms a frequency domain signal into a random time domain signal, throughout a frequency spectrum, and is used to create OFDM symbols after coding and base band modulation, which is then used for pass band modulation. A time-domain CP of duration N_{CP} samples is set to surpass the maximum channel delay spreading (L_h) and is injected at the start of each OFDM symbol by duplicating the final N_{CP} samples of the IFFT output x and attaching them to the start of x to generate symbols $\tilde{x}$ =$[x_{N-N_{CP}}, x_{N-N_{CP}+1},\ldots,x_{N,}x_o, x_1, \ldots, x_{N-1}]$, that are transmitted and have length N_t = $N + N_{CP}$ samples [19]. This removes ISI between successive OFDM signals in channels. These carriers travel through a variety of fading channels, each of which adds its own noise at the receiving which is produced the signal shown in equation (1), where α is the complex RV describing the impulse response parameters in the domain of time of a multipath fading channel and w is the additive white noise. It has already been said that the Rayleigh distribution is used to model the multipath fading channel for wireless systems, that PDF will be spread out according to equation (2), and that the Nakagami-m distribution is shown by equation (5). After the removal of the guard interval, the OFDM carrier is demodulated by performing a Fast Fourier Transform (FFT), which transforms the signal from the time domain back into the frequency domain. The complex received signal at the receiver, as expressed in (1), can be represented as follows in the frequency domain:[18, 27]

$$Y^I + jY^Q = (A^I + jA^Q).(X^I + jX^Q) + W^I + \mathrm{j}W^Q \tag{11}$$

Where, in the frequency domain, Y, A, X, and W stand in for, respectively, the complex received signal, the transfer function of the complex fading channel, the complex modulated signals, and the AWGN. According to the Central Limit Theorem (CLT), the distribution of the real component and the distribution of the imaginary part approach a Gaussian distribution after FFT operation with mean equal to zero, =0, and variance depend on the channel used. In the case of Rayleigh fading channel, the p(A^I) and p(A^Q) can be expressed as [20, 25]

$$f_A(A^I) = \frac{1}{\sqrt{2\pi\sigma_h^2}} \exp\left(-\frac{(A^I)^2}{2\sigma_h^2}\right), \quad -\infty \le A^I < \infty \tag{12}$$

$$f_A(A^Q) = \frac{1}{\sqrt{2\pi\sigma_h^2}} \exp\left(-\frac{(A^Q)^2}{2\sigma_h^2}\right), \quad -\infty \le A^Q < \infty \tag{13}$$

While, in the case of Nakagami-m fading channel, the p(A^I) and p(A^Q) can be expressed as [11, 20, 21, 23]

$$f_A(A^I) = \frac{1}{\sqrt{2\pi\sigma_N^2}} \exp\left(-\frac{(A^I)^2}{2\sigma_N^2}\right), \quad -\infty \le A^I < \infty \tag{14}$$

$$f_A(A^Q) = \frac{1}{\sqrt{2\pi\sigma_N^2}} \exp\left(-\frac{(A^Q)^2}{2\sigma_N^2}\right), \quad -\infty \le A^Q < \infty \tag{15}$$

Where, $\sigma_N^2 = \Omega\left(1 - \frac{1}{m}\left(\frac{\Gamma(m+\frac{1}{2})}{\Gamma(m)}\right)^2\right)$ [11, 21]. Hence, the magnitude of the channel frequency response, |A|=$\sqrt{(A^I)^2 + (A^Q)^2}$, will fallow the Rayleigh distribution in the frequency response for both channels.

In a 4-QAM system, the complex received noisy signal is denoted by Y in the frequency domain expressed in (11), and the set of all possible modulated symbols X is denoted by C = {C_1, C_2, C_3, C_4 }. The bit error rate (BER) in the AWGN can be expressed as

$$P_b^{AWGN} = Q\left(\sqrt{\frac{2E_b}{No}}\right) \tag{16}$$

A different form of Eq. (16) is as follows.

$$P_b^{AWGN} = \frac{1}{2} erfc\left(\sqrt{\frac{E_b}{No}}\right) \tag{17}$$

And the BER over Rayleigh fading channel can be expressed as

$$P_b^{Rayleigh} = \frac{1}{2}\left[1 - \left(\frac{\sqrt{\frac{E_b}{2\sigma_w{}^2}}}{\sqrt{1+\frac{E_b}{2\sigma_w{}^2}}}\right)\right] \quad (18)$$

5. BER computation over Nakagami-m Fading Channel

To determine the BER of QAM-OFDM over Nakagami-m fading channel in AWGN. The effective bit energy to noise ratio is, $\gamma = \frac{|A|^2 E_b}{2\sigma_w{}^2}$. Therefore, for a given value of A, the bit error probability is

$$P_{b|A} = \frac{1}{2} erfc(\sqrt{\gamma}) \quad (19)$$

We know from our consideration of the chi-square random variable that it has two degrees of freedom if it is a Rayleigh distributed random variable expressed as, $p(\gamma) = \frac{1}{E_b/2\sigma_w{}^2} e^{-\frac{\gamma}{E_b/2\sigma_w{}^2}}$, $\gamma \geq 0$. Therefore, the BER can be computed as:

$$P_b^{Nakagami-m} = \int_0^\infty \frac{1}{2} erfc(\sqrt{\gamma})\, p(\gamma) d\gamma = \int_0^\infty \frac{1}{2} erfc(\sqrt{\gamma})\, \frac{1}{E_b/2\sigma_w{}^2} e^{-\frac{\gamma}{E_b/2\sigma_w{}^2}} d\gamma = \frac{1}{2}\left[1 - \left(\frac{\sqrt{\sigma_N^2 \frac{E_b}{2\sigma_w{}^2}}}{\sqrt{1+\sigma_N^2 \frac{E_b}{2\sigma_w{}^2}}}\right)\right] \quad (20)$$

6. Simulation Results and Analysis

The performance of NR- LDPC- QAM-OFDM system in terms of BER for different block lengths and variable code rates over different communication channels: Rayleigh channel, and Nakagami-m, have been examined and compared with the performance of uncoded QAM-OFDM system. Parmeters defined in Table 2 are used to utilize above mentioned channels.

Table 2. Simulation Parameters

Modulation	QAM
No. of sub-carriers	64
No. of Block length	1000
Channel model	Frequency selective Rayleigh fading channel Frequency selective Nakagami-m fading channel
Noise	AWGN
Code rate	1/2 and 1/3

The BER performance of NR- LDPC- QAM-OFDM Scheme for two base graphs are comared with respective uncoded QAM-OFDM under AWGN, and fading channel Fig. 3 and 4, show the performance of BER of LDPC-OFDM systems for code rate 1/3 and 1/2, with varied parameter n. Which is compared for block length n = 1024 bits, and n=128 and BER = 10^{-6} as error rate target. It can be seen from the figures, the performance of BG2 outperforms BG1 in the case n=128 and the performance of BG1 outperforms BG2 in the case n= 1024 and the performance gap between them is significantly reduced to 0.3 dB compared to 1.1 dB in the case of the short block length n=128. According to the findings, the possible range of blocks is between ten thousand and one thousand. Therefore, the total number of bits is equal to 10000 *Zc. The layered Min Sum(MS) approach has been put into action, and success has been attained with fewer iterations comparing with SPA and MSA.

According to the findings, results indicate that the NR- LDPC- QAM-OFDM system which is designed enables a considerable improvement over the un-coded system about 9.5dB at 10^{-6} BER for block length 1024, when used Basegraph1, and achieve improvement about 6.5dB at 10^{-6} BER for block length 128, under AWGN model and the performance have a little degradation when employed Basegraph 2.

The variances of AWGN channel model are estimated using SNR values. In the case of fading presence, a fading channel block was accompanied by the AWGN channel block that had previously been used. Fig. 5, and Fig. 6, show the performance of NR-LDPC-4QAM -OFDM of both base graphs system over Rayleigh fading channel compared to the theoretical BER performance of the UOFDM system.

In this simulation, can be demonstrated that the theoretical BER and the experimental BER correspond well for Uncoded OFDM, over Rayleigh channel coding. Ultimately, it is determined that channel coding has the potential to enhance BER performance of the system. Hence a coding gain is needed for the coded OFDM with LDPC decoding to obtain a bit error rate of 10^{-6}, as is evident from the data shown in Table 3. Each simulation was run for a total of 100 frames, and the process was kept going until a BER value of 10^{-6} was attained, number of transmitted bits per frame10^7.

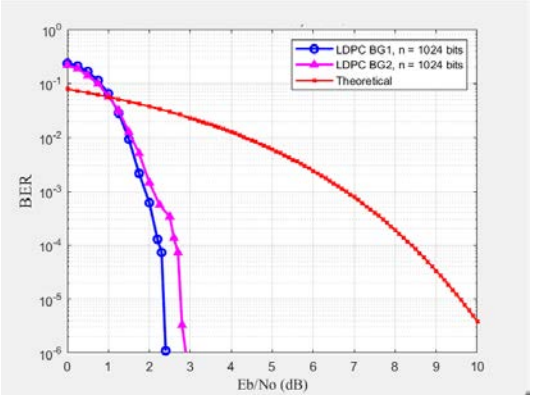

Fig.3. BER of LDPC-OFDM systems at R=1/3

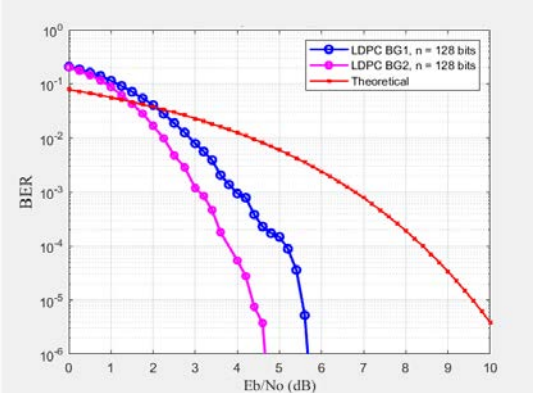

Fig.4. BER of LDPC-OFDM systems at R=1/2

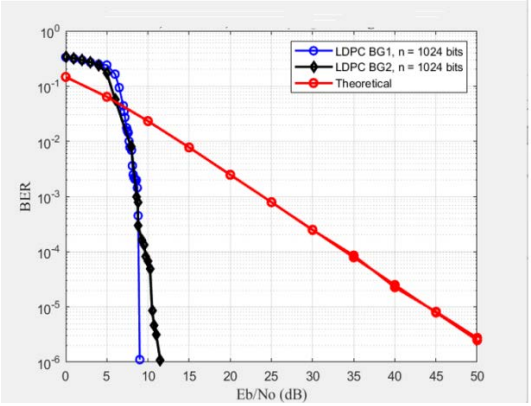

Fig.5. BER of LDPC-OFDM systems (n=1024)

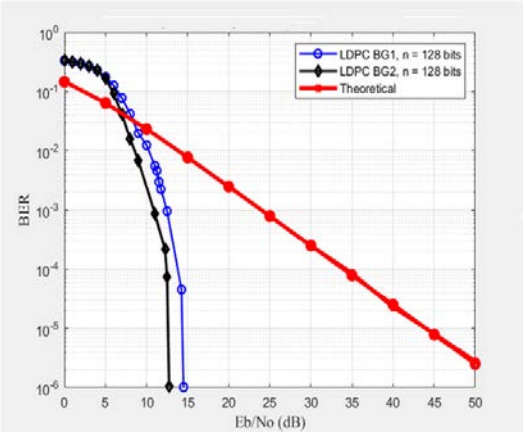

Fig.6. BER of LDPC-OFDM systems (n=128)

Table 3. coded gain of two base graphs over Rayleigh fading channel (n=1024)

BER	E_b/N_0, dB				
	BG1	BG2	Uncoded system	Gain1	Gain2
10^{-3}	8.4 dB	8.8 dB	24 dB	15.6 dB	15.2 dB
10^{-4}	8.8 dB	9.25 dB	34 dB	25.2 dB	24.75dB
10^{-5}	9 dB	10.5 dB	44 dB	35 dB	33.5 dB
10^{-6}	9 dB	11.5 dB	55 dB	46 dB	43.5 dB

As can be observed in the Figure, at a BER of 10^{-4}, BG1 of LDPC provides around 15.6 dB more coding gain than for UOFDM system under Rayleigh fading channel. Additionally, BG1for LDPC code performs superior to BG2 of LDPC code at approximately greater than 10^{-4}. Furthermore, the findings of the Monte Carlo simulation techniques exhibits closely match to the theoretical performance of the UOFDM system under the same characteristics.

Fig. 7, and Fig. 8, show the performance of NR-LDPC-QAM -OFDM of both base graphs system over Nakagami-m fading channel compared to the theoretical BER performance of the UOFDM system.

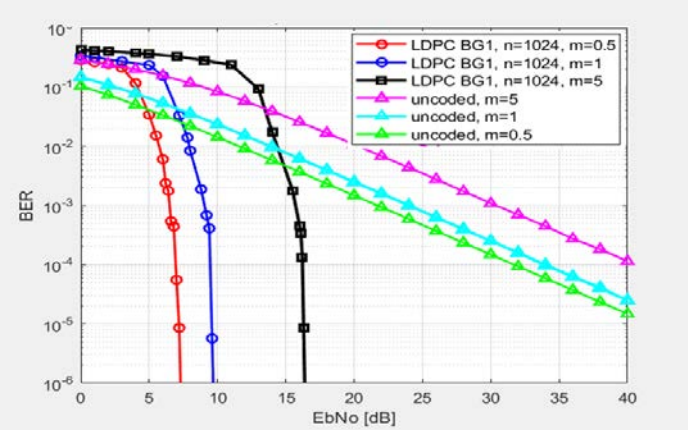

Fig.7. BER performance for BG1 of LDPC / 4QAM-OFDM over Nakagami-m fading channel

The dramatic improvement in system performance achieved about through the use of LPDC-OFDM over UOFDM, with the latter yielding greater coding improvements. As can be observed in the Fig.7, and 8, when shaping factor (m=0.5) at a BER of 10^{-4}, BG1 of LDPC provides around 25 dB more coding gain and BG2 provides around 24.6 dB more coding gain than for UOFDM system, over nakagami-m fading channel. Additionally, BG1 for LDPC code performs superior to BG2 of LDPC code at approximately greater than 10^{-4}. Furthermore, the findings of the Monte Carlo simulation techniques exhibits closely match to the theoretical performance of the UOFDM system under the same characteristics.

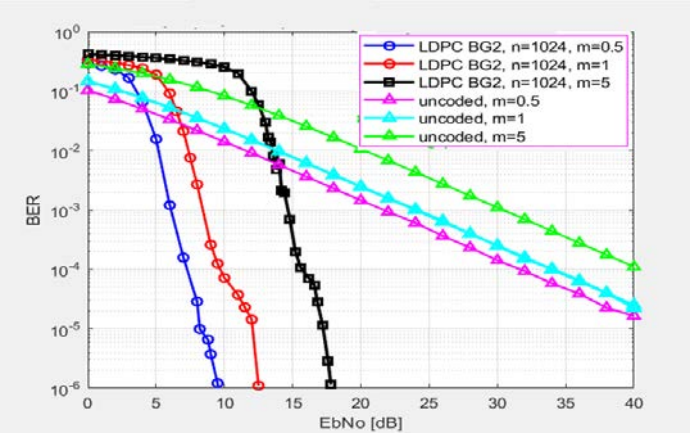

Fig.8. BER performance for BG2 of LDPC / 4QAM-OFDM over Nakagami-m fading channel

It is also evident that, for the LMSA decoding algorithm, the coding gain is substantially larger with smaller shaping factor of nakagami-m fading channel, even for the scenario where the maximum number of iterations is lowered by eight times. Table 4 provides numerical examples for evaluation and Coded Gain(CGs) for variants of

possible outcomes of the shaping parameter (m). For decreasing values of m, the system performs better, but the coding gain decreases since the signal strength fluctuates less compared to the Rayleigh fading case when m=1.

Table 4. Provides numerical examples

Fading (shaping) factor	m=0.5		m=1		m=5		CG at m =1		
BER	BG1	BG2	BG1	BG2	BG1	BG2	Uncoded	Gain1	Gain2
10^{-3}	6.8 dB	7dB	8 dB	8.4 dB	16dB	14dB	24 dB	17 dB	16.6 dB
10^{-4}	7 dB	7.5dB	9 dB	9.4 dB	16.5	16dB	34 dB	25 dB	24.6 dB
10^{-5}	7.5 dB	8.5 dB	9.2 dB	12dB	17dB	17.2	44 dB	34.8 dB	32 dB
10^{-6}	7.5 dB	9dB	9.2 dB	12.5 dB	17dB	17.6	55 dB	45.8 dB	42.5 dB

7. Conclusions

In this work, the effectiveness of the NR- LDPC- OFDM system takes into consideration, the multipath fading channel . A Rayleigh distribution and the Nakagami-m model are used to account for the many causes that contribute to the distorted signal in the channel. Through the use of Monte Carlo simulations, we find that QAM constellation NR-LDPC-OFDM with total belief LLRs achieved high coding gain compared to the uncoded OFDM in a AWGN under Rayleigh and Nakagami-m fading channel conditions. Moreover, Under low signal-to-noise situations, the NR-LDPC can reduce the number of decoding rounds required for correcting channel errors by 16-24%. The NR-LDPC code work efficiently when the base matrix have a large expansion factor. So that the results do seem to indicate that the performance of NR-LDPC codes improves with increasing block length and degrades with increasing code rate. The coding rate and block length of BG1 are superior to those of BG2, which is why it is used here. For Rayleigh fading find that, the performance improvement of NR_LDPC with BG1 over BG2 is more obviously, and that increasing the codeword length marginally improves system performances.

A variety of shaping factors (m=0.5, 1and 5) have been tested in simulations of the NR-LDPC-QAM-OFDM system operating in AWGN under the Nakagami-m fading channel. The results show that when (m<1), the Nakagami-m fading channel has higher coding gain than the Rayleigh fading channel for all values of Eb/No.

Finally, it is clear that the used decoding technique(LMSA) has a significant effect, and that longer codewords enhance performance, however this benefit is perceptible specially at lower BER levels.

References

[1] M. Maksimovi and M. Forcan, “Application of 5G Channel Coding Techniques in Smart Grid : LDPC vs . Polar coding for Command Messaging,” *7th Int. Conf. Electr. Electron. Comput. Eng.*, pp. 746–751, 2020.

[2] D. Čarapić and M. Maksimović, “A Comparison of 5G Channel Coding Techniques,” *Ijeec - Int. J. Electr. Eng. Comput.*, vol. 4, no. 2, pp. 71–82, 2020, doi: 10.7251/ijeec2002071m.

[3] Y. Fang, G. Bi, Y. L. Guan and F. C. M. Lau, "A Survey on Protograph LDPC Codes and Their Applications," in IEEE Communications Surveys & Tutorials, vol. 17, no. 4, pp. 1989-2016, Fourthquarter 2015, doi: 10.1109/COMST.2015.2436705.

[4] S. Cheng, “Comparative Study on 5G Communication Channel Coding Technology,” vol. 87, no. November 2016, pp. 74–77, doi: 10.2991/icmeit-19.2019.13.

[5] M. Ben Abdessalem, A. Zribi, T. Matsumoto, E. Dupraz, and A. Bouall, “LDPC-based Joint Source Channel Coding and Decoding Strategies for single relay cooperative communications,” no. November, 2019, doi: 10.1016/j.phycom.2019.100947.

[6] J. Malhotra, “Performance Evaluation of Channel Codes for High Data Rate Mobile Wireless System”, International Journal of Wireless and Microwave Technologies, vol.5, no.4, pp.24-36, 2015.

[7] Y. Jiang, A. Ashikhmin, and N. Sharma, “LDPC Codes for Flat Rayleigh Fading Channels with Channel Side Information,” vol. 56, no. 8, pp. 1207–1213, 2008..

[8] A. Anbalagan , S. Subramani, C. Kamalanathan, and S. Panda″ Performance analysis of short length low density parity check codes," *I*nt J Speech Technol 24, 615–624,2021. doi:org/10.1007/s10772-021-09815-1.

[9] Y. Fang, G. Han, G. Cai, F. C. M. Lau, P. Chen and Y. L. Guan, "Design Guidelines of Low-Density Parity-Check Codes for Magnetic Recording Systems," in IEEE Communications Surveys & Tutorials, vol. 20, no. 2, pp. 1574-1606, Secondquarter 2018, doi: 10.1109/COMST.2018.2797875.

[10] S. A. Ghauri, M. E. U. Haq, M. Iqbal and J. U. Rehman, "Performance Analysis of LDPC Codes on Different Channels," 2014 Eighth International Conference on Next Generation Mobile Apps, Services and Technologies, 2014, pp. 235-240, doi: 10.1109/NGMAST.2014.34.

[11] G. A. Al-rubaye, C. C. Tsimenidis, and M. Johnston, "Performance evaluation of T-COFDM under combined noise in PLC with log-normal channel gain using exact derived noise distributions." *IET Communications* 13.6 (2019): 766-775.

[12] B. Tahir, S. Schwarz and M. Rupp, "BER comparison between Convolutional, Turbo, LDPC, and Polar codes," 2017 24th International Conference on Telecommunications (ICT), 2017, pp. 1-7, doi: 10.1109/ICT.2017.7998249.

[13] 3rd Generation Partnership Project; Technical Specification Group Radio Access Network; NR; Multiplexing and channel coding (Release 15), 2019.

[14] Multiplexing and Channel Coding, document TS 38.212 V15.0.0, 3GPP, Dec. 2017.

[15] D. S. Shafiullah, M. R. Islam, Mohammad Mostafa Amir Faisal and I. Rahman, "Optimized Min-Sum decoding algorithm for

Low Density PC codes," 2012 14th International Conference on Advanced Communication Technology (ICACT), 2012, pp. 475-480.
[16] W. Zhou and M. Lentmaier, "Generalized two-magnitude check node updating with self correction for 5G LDPC codes decoding," in Proc. 12th Int. ITG Conf. Syst., Commun. Coding, Rostock, Germany, Mar. 2019, pp. 1–6.
[17] M.K. Roberts, R. A. Jayabalan, "Modified Optimally Quantized Offset Min-Sum Decoding Algorithm for Low-Complexity LDPC Decoder," Wireless Pers Commun 80, 2015, 561–570. doi: org/10.1007/s11277-014-2026-2.
[18] K. Sun and M. Jiang, "A hybrid decoding algorithm for low-rate LDPC codes in 5G," in Proc. 10th Int. Conf. Wireless Commun. Signal Process. (WCSP), Hangzhou, China, Oct. 2018, pp. 1–5.
[19] X. Wu, M. Jiang, and C. Zhao, "Decoding optimization for 5G LDPC codes by machine learning," IEEE Access, vol. 6, pp. 50179–50186, 2018.
[20] G. A. Al-rubaye, C. C. Tsimenidis, and M. Johnston, "Non-binary LDPC coded OFDM in impulsive power line channels." *2015 23rd European Signal Processing Conference (EUSIPCO)*. IEEE, 2015.
[21] G. A. Al-rubaye, C. C. Tsimenidis, and M. Johnston, "Low-density parity check coded orthogonal frequency division multiplexing for PLC in non-Gaussian noise using LLRs derived from effective noise probability density functions," pp. 2425–2432, 2017, doi: 10.1049/iet-com.2017.0265.
[22] H. Zarrinkoub, Understanding LTE with MATLAB: from mathematical foundation to simulation, performance evaluation and implementation, John Wiley & Sons, Ltd, 2014.
[23] G. A. Al-rubaye, C. C. Tsimenidis, and M. Johnston, "Improved performance of TC-OFDM-PLNC for PLCs using exact derived impulsive noise pdfs." *2017 IEEE International Conference on Communications Workshops (ICC Workshops)*. IEEE, 2017.
[24] Samarendra Nath Sur, Debjyoti Ghosh,"Channel Capacity and BER Performance Analysis of MIMO System with Linear Receiver in Nakagami Channel", International Journal of Wireless and Microwave Technologies, vol.3, no.1, pp.26-36, 2013.
[25] G. A. Al-rubaye, "Performance analysis of M-ary OQAM/FBMC with impact of nonlinear distortion over compound Rician K-factor unshadowed/κ− μ shadowed fad ing channels." *IET Communications* 15.1,pp. 60-77 , 2021.
[26] P. Chai and L. Zhang, "Indoor radio propagation models and wireless network planning," 2012 IEEE International Conference on Computer Science and Automation Engineering (CSAE), 2012, pp. 738-741, doi: 10.1109/CSAE.2012.6272872.
[27] S. Sharma, "A Simulation Model for Nakagmi-m Fading Channel with m > 1," vol. 6, no. 10, pp. 298–305, 2015.
[28] Sanjiv Kumar, P. K. Gupta, G. Singh, D. S. Chauhan,"Performance Analysis of Rayleigh and Rician Fading Channel Models using Matlab Simulation", International Journal of Intelligent Systems and Applications, vol.5, no.9, pp.94-102, 2013.
[29] Zachaeus K. Adeyemo, Samson I. Ojo, Simeon B. Ebinaiye, Olasunkanmi F. Oseni, "Development of a Hybridized Diversity Combiner over Nakagami Fading Channel", International Journal of Information Engineering and Electronic Business(IJIEEB), Vol.11, No.3, pp. 45-53, 2019. DOI: 10.5815/ijieeb.2019.03.06
[30] R. Bose, "Information Theory, Coding and Cryptography", 3rd Edition, McGraw Hill, July 2, 2016.
[31] Multiplexing and Channel Coding, document TS 38.212 V15.0.0, 3GPP, Dec. 2018.
[32] O.Bancalo. G.Kolmban, D. Declercq, and V.Savin," Code-design density for efficient layered LDPC decoders with bank memory organization,". Microprocessors and Microsystems:, 63 , 216-225, Nov. 2018. doi.org/10.1016/j.micpro.2018.09.011.
[33] S. Ahmadi, 5G NR Architecture, Technology, Implementation, and Operation of 3GPP New Radio Standards, Academic Press, Elsevier, 2019.
[34] Ad-Hoc chair (Nokia). Chairman's Notes of Agenda Item 7.1.4. Channel Coding. 3GPP TSG RAN WG1 Meeting AH 2, R1-1711982 (2017). Available Online: https://portal.3gpp.org/ngppapp/CreateTdoc.aspx? mode=view & contributionId=805088 (accessed on 20 February 2021).
[35] S M Shamsul Alam, Anamika Saha, " Performance Analysis of FBMC over OFDM for High Data Rate MIMO Configurations", International Journal of Wireless and Microwave Technologies, Vol.11, No.4, pp. 20-33, 2021.

Authors' Profiles

Mohammed Hussein Ali is a lecturer in the Information and Communications Engineering Department, Faculty of Information Engineering, Al-Nahrain University. He holds his B.Sc degree from the College of Engineering, University of Baghdad, in 2004, and received his M.Sc. in Electronics and Communications Engineering from Al-Mustansiriyah University in 2010, and is currently a Ph.D. student in Communications Engineering at Al-Mustansiriyah University. His areas of interest are cellular network communications, coding techniques, and signal processing for wireless communications.

Dr. Ghanim A. Al-Rubaye is an Asst. Prof. in the Electrical Engineering Department, Faculty of Engineering, Mustansiriyah University, Baghdad, Iraq. He received his M.Sc. in Electronics and Communications from Al-Mustansiriya University, Baghdad, Iraq, in 1999. He received his PhD from the School of Electrical and Electronics Engineering, Newcastle University, Newcastle Upon Tyne, U.K, in 2017. His research focuses on wired/wireless communications on coded systems, OFDM systems, fading and power line communication channels, channel modelling and receiver design.

How to cite this paper: Mohammed Hussein Ali, Ghanim A. Al-Rubaye, "Performance Analysis of 5G New Radio LDPC over Different Multipath Fading Channel Models", International Journal of Computer Network and Information Security(IJCNIS), Vol.15, No.4, pp.1-12, 2023. DOI:10.5815/ijcnis.2023.04.01